JOURNAL OF VIROLOGY, Jan. 1987, p. 177–184
0022-538X/87/010177-08$02.00/0
Copyright © 1987, American Society for Microbiology
Vol. 61, No. 1

Noncoding Region between the *env* and *src* Genes of Rous Sarcoma Virus Influences Splicing Efficiency at the *src* Gene 3′ Splice Site

C. MARTIN STOLTZFUS,[1]* SUSAN K. LORENZEN,[1] AND STANTON L. BERBERICH[2]

Department of Microbiology[1] and Program in Genetics,[2] University of Iowa, Iowa City, Iowa 52242

Received 16 June 1986/Accepted 22 September 1986

Viral RNA and proteins in chicken embryo fibroblasts infected with different cloned variants of the Prague strain Rous sarcoma virus (RSV) were analyzed. The ratio of immunoprecipitated pp60^{src} to the *gag* gene product p27 in Prague A (PrA) and Prague B (PrB) RSV-infected cells was two to three times that in Prague C (PrC) RSV-infected cells. A significant increase in the steady-state ratio of spliced 2.7-kilobase *src* gene mRNA to unspliced 9.3-kilobase genome-size RNA was observed in PrA- and PrB- compared with PrC-infected cells, consistent with the differences in the ratios of the *gag* to *src* gene protein products. Similar results were obtained when hybrid-selected RNA, which had been labeled for 3 h with [^{3}H]uridine, was analyzed on formaldehyde-agarose gels, suggesting that the observed differences were due to splicing rather than RNA stability. Recombinant plasmids from infectious molecular clones of PrA and PrC were constructed to localize the regions responsible for the effects on *src* gene splicing. The substitution in place of the corresponding PrA region of the 262-base-pair region between the *env* gene and the *src* gene coding sequences from the PrC clone into the infectious PrA plasmid conferred the low *src* splicing efficiency of the PrC strain. The nucleotide sequence of this region of the PrA plasmid was determined and compared with the sequence of the PrC strain. Only four nucleotide differences were found; two changes were within the intron sequence, and two were in the exon sequence. The possible role of these differences in determining the extent of viral RNA splicing is discussed.

Retrovirus RNA processing is unusual in that roughly half the viral RNA transcripts are transported as unspliced RNA to the cytoplasm of infected cells. The unspliced RNA serves as genome RNA and also as mRNA for the synthesis of *gag* and *pol* gene products. At least part of the spliced RNA is used as mRNA for the *env* gene product. Since *gag*, *pol*, and *env* gene products are each required for infectious virus production, the replication of these viruses is dependent on the maintenance of a balance between spliced and unspliced RNA. The mechanism by which a portion of the viral RNA escapes splicing is not understood (for a review, see reference 35).

To further elucidate the possible regulatory role of viral and cellular proteins, as well as the role of RNA modifications in regulating retrovirus splicing, we investigated the splicing of viral mRNAs in Rous sarcoma virus (RSV)-infected chicken embryo fibroblasts (CEF). Two spliced mRNAs were produced during infection with RSV, the 5.4-kilobase (kb) *env* gene mRNA and the 2.7-kb *src* gene mRNA. Both mRNAs are generated by single splicing events (1) in which a 398-base 5′ leader exon (7) is spliced to alternative acceptor sites at nucleotides 5078 and 7054 for the *env* and *src* gene mRNAs, respectively (5, 26, 32). We found striking differences in the ratios of spliced *src* gene mRNA to unspliced genome RNA when several different strains of RSV were compared, and these differences have been correlated with relative levels of pp60^{src} in the infected cells. The levels of *env* mRNA in cells infected by these strains, however, were similar. Our evidence suggests that the differences in splicing of *src* mRNA are due to RNA splicing rather than RNA turnover. Moreover, we localized the sequences responsible for this effect to the noncoding region between the *env* and *src* genes.

* Corresponding author.

MATERIALS AND METHODS

Viruses, cells, and plasmids. CEF were prepared from C/E *chf*$^-$ *gs*$^-$ embryonated eggs obtained from SPAFAS, Inc., Norwich, Conn., and were grown in medium 199 with 10% tryptose phosphate broth and 5% calf serum (SGM). Infectious Prague A (PrA) RSV plasmid pJD100 was generously provided by J. Thomas Parsons, University of Virginia, Charlottesville. Infectious Prague C (PrC) RSV plasmid pATV-8 (11) was obtained from John Coffin, Tufts University, Medford, Mass. Cloned Prague B (PrB) RSV was a gift from Allan Tereba, St. Jude Children's Research Hospital, Memphis, Tenn.

Transfection procedures. Transfection was carried out by the calcium phosphate precipitation method (6). In the case of pATV-8 in which the viral genome was permuted, the plasmid was partially digested with *Hin*dIII and religated to form concatemers. Plasmid DNA (100 to 1,000 ng) and 20 μg of salmon sperm DNA were added to 0.48 ml of 0.25 M $CaCl_2$ solution. To this solution was added 0.5 ml of 2× HEPES (*N*-2-hydroxyethylpiperazine-*N*′-2-ethanesulfonic acid)-buffered saline, pH 7.05, and the mixture was incubated for 30 min at room temperature. This was then pipetted onto cultures of CEF containing 2×10^6 cells per plate. After 30 min at room temperature, 10 ml of medium 199 containing 10% calf serum, 10% tryptose phosphate broth, and 1% heat-inactivated chicken serum was added, and the treated cells were incubated for 3 to 4 h at 37°C. At this time the medium was removed, and the cultures were incubated with 3 ml of 30% dimethyl sulfoxide in HEPES-buffered saline for 4 min. They were then washed with 3 ml of SGM containing 1% chicken serum, and then 10 ml of SGM was added. Transformation was apparent after several days. The cells were passaged several times to ensure complete infection.

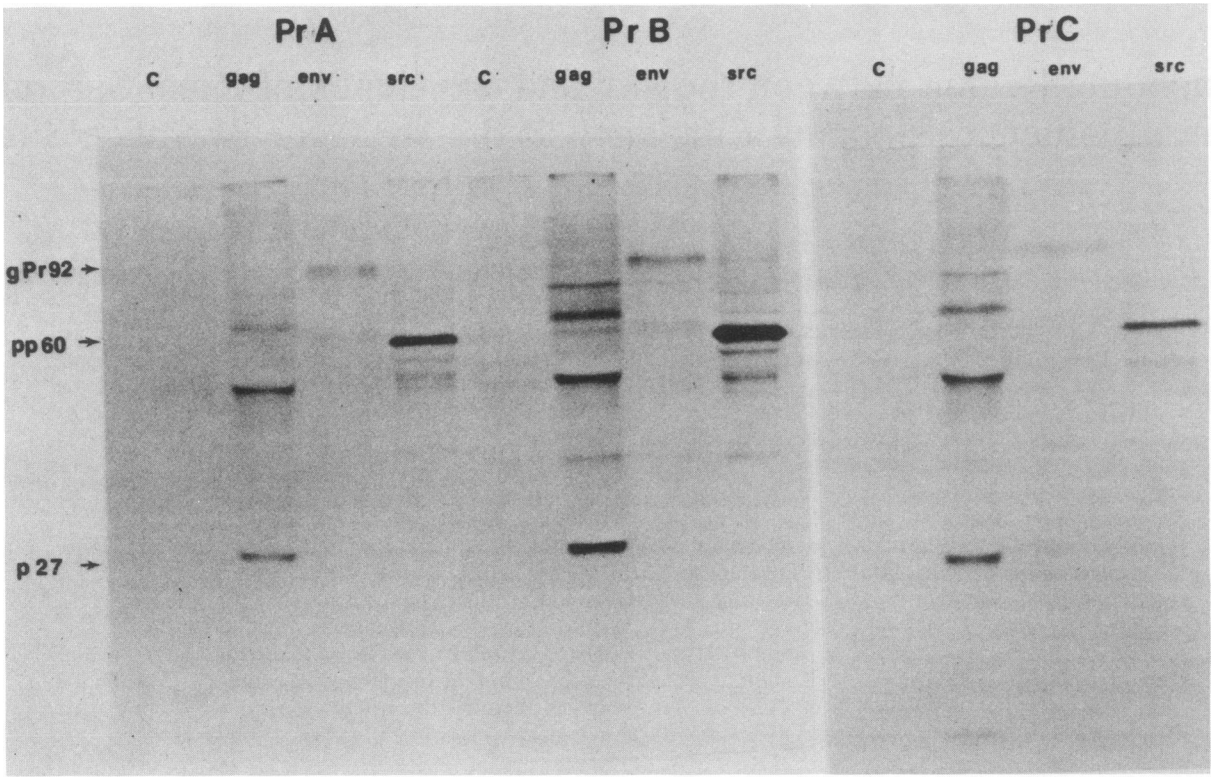

FIG. 1. Virus-specific polypeptide synthesis in RSV-infected cells. Cells infected with PrA, PrB, and PrC RSVs were labeled for 5 h with [^{3}H]methionine, total protein was isolated, and virus-specific polypeptides were immunoprecipitated from samples of 5×10^5 cpm of total protein with appropriate antisera by methods described in the text. The virus-specific proteins were analyzed by electrophoresis at 120 V on 10% sodium dodecyl sulfate-polyacrylamide gels. The immunoprecipitates with antiserum to the *gag* protein p27, to the *env* proteins, and to the *src* gene protein pp60^{src} are indicated. The *env* antiserum immunoprecipitates the envelope protein precursor gPr92^{env}. The C lanes are controls with normal antiserum.

Radioactive labeling of polypeptides in virus-infected cells. Three 100-mm-diameter plastic petri dishes containing cells infected with either PrA, PrB, or PrC RSV were treated for 12 h with Earle minimal essential medium containing 10 μM methionine, 10% tryptose phosphate broth, and 5% calf serum (low-methionine medium). The plates were labeled with 25 μCi of [^{35}S]methionine per ml for 5 h in 5 ml of low-methionine medium. The medium was then removed, and the cells were washed two times with ice-cold 140 mM NaCl–5 mM KCl–0.6 mM Na_2HPO_4–5.5 mM glucose–25 mM Tris (pH 7.2) and suspended in 1 ml of RIPA buffer containing 1% (vol/vol) aprotinin (27). The cells were disrupted by Dounce homogenization and centrifuged at 25,000 rpm for 30 min in a type 65 rotor (Beckman Instruments, Inc., Fullerton, Calif.). The supernatants were removed, and 0.2-ml samples were quick-frozen in a dry ice-acetone bath. Determinations of incorporation of [^{35}S]methionine into protein were carried out by scintillation counting of hot 5% trichloroacetic acid-precipitable material. Protein analyses were carried out by the procedure of Lowry et al. (16). The specific activities were approximately 6×10^3 cpm/μg of protein.

Immunoprecipitation of viral polypeptides. Appropriate amounts of protein (approximately 5×10^5 cpm) were added in a total volume of 50 μl to 1.5-ml plastic centrifuge tubes. To each tube was added 15 μl of normal rabbit or normal goat serum as appropriate. Immunoprecipitation with *Staphylococcus aureus* was carried out by the methods of Kessler (12) as described by Stoltzfus and Dane (29). The supernatants containing the virus-specific proteins were loaded onto sodium dodecyl sulfate-polyacrylamide gels by the procedures described by Laemmli (13). The gel was then prepared for fluorography as described previously (28).

Labeling of RNA with [^{3}H]uridine, hybrid selection of viral RNA, and electrophoresis on formaldehyde-agarose gels. Petri dishes containing CEF infected with various virus strains were labeled with [^{3}H]uridine (50 μCi/ml) for 3 or 12 h. After the labeling period, the cells were washed with ice-cold 140 mM NaCl–5 mM KCl–0.6 mM Na_2HPO_4–5.5 mM glucose–25 mM Tris (pH 7.2), and RNA was purified by the guanidine hydrochloride procedure of Strohman et al. (31). Virus-specific RNA was hybrid selected essentially by the procedure described by Stoltzfus and Dane (29). Approximately 25,000 cpm of each sample was loaded onto a formaldehyde-agarose gel. The gel was run overnight, and on the following day the RNA was transferred to nitrocellulose by blotting. After drying under vacuum for 4 h at 70°C, the filter was dipped in molten 2-methylnaphthalene containing 0.4% (wt/vol) diphenyloxazole and exposed to X-ray film.

Cloning procedures and restriction enzyme digestions. Cloning techniques were carried out by standard methods described by Maniatis et al. (17). Restriction enzyme digestions were carried out by the specifications of the suppliers.

Northern blot analysis of RNA. Northern blot analysis of RNA on formaldehyde-agarose gels was carried out as described previously (17). ^{32}P-labeled probes were prepared by the nick translation technique of Rigby et al. (23).

DNA sequence analysis. Sequence determination was per-

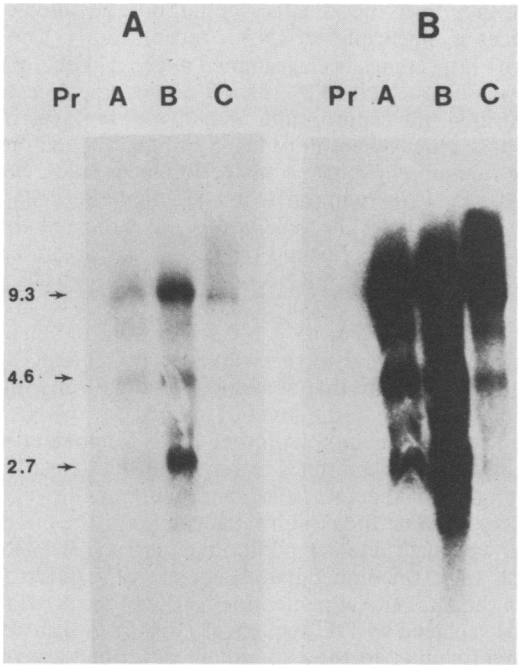

FIG. 2. Northern blot hybridization analysis of virus-specific RNA in RSV-infected cells. A 10-μg amount of total RNA from PrA, PrB, and PrC was electrophoresed on formaldehyde-agarose gels by the procedures in the text. The RNA was transferred to nitrocellulose and hybridized to 2×10^6 cpm of ^{32}P-labeled probe (3.1-kb *Eco*RI fragment spanning nucleotides 6144 to 9238). Autoradiography was carried out for either 48 h (A) or 7 days (B).

formed by the chemical degradation method (18). Both strands of the *Xba*I-*Bgl*II fragment (nucleotides 6861 to 7736) from pJD100 were labeled at the *Xba*I site and sequenced. The 5′ end was labeled with [γ-^{32}P]ATP by using T4 polynucleotide kinase, and the 3′ end was labeled with [α-^{32}P]dCTP by using the Klenow fragment of *Escherichia coli* DNA polymerase (Boehringer Mannheim Biochemicals, Indianapolis, Ind.).

Materials. [5,6-^{3}H]uridine (44 Ci/mmol), L-[^{35}S]methionine (1,000 to 1,500 Ci/mmol), and ^{32}P-labeled deoxyribonucleotides and ribonucleotides (2,000 Ci/mmol) were purchased from Amersham Corp., Arlington Heights, Ill. Guanidine hydrochloride and aprotinin were obtained from Sigma Chemical Co., St. Louis, Mo. Actinomycin D (dactinomycin) was obtained from Stanley Perlman, University of Iowa, and was a gift from Merck Sharpe & Dohme, West Point, Pa. Antiserum to pp60^{src} was a generous gift from J. Thomas Parsons, University of Virginia. Antiserum to virion protein p27 was obtained from the Division of Cause and Prevention, National Cancer Institute, Bethesda, Md. Antiserum to the viral glycoproteins gp85 and gp37 was obtained by injection of purified glycoproteins from B77 virions into rabbits. All antisera were polyclonal. Restriction enzymes were purchased from Bethesda Research Laboratories, Inc., Gaithersburg, Md., or New England BioLabs, Inc., Beverly, Mass.

RESULTS

Accumulation of viral polypeptides in infected cells. We observed in preliminary studies that CEF infected with a cloned isolate of PrC RSV were less rounded and considerably more adherent to plastic petri dishes than were cells infected with cloned isolates of PrA and PrB RSVs. To understand the molecular basis for these phenotypic differences, we first measured the levels of the various viral proteins in infected cells. Cell cultures were infected with PrB RSV virus or transfected with cloned PrA and PrC RSV DNAs. The cells were passaged several times until they appeared to be completely transformed. Subconfluent cultures of infected cells were labeled for 5 h with [^{3}H]methionine. Cell extracts were prepared, and equal amounts of protein from each extract were immunoprecipitated with excess antiserum to the *gag* gene protein p27, the *env* gene proteins gp85 and gp37, and the transforming protein pp60^{src}. The immunoprecipitates were analyzed on sodium dodecyl sulfate-polyacrylamide gels. The results (Fig. 1) indicated that the PrB RSV-infected cells contained a larger amount of total viral protein than did cells infected with either the PrA or the PrC strain. It was also evident from these gels that there were considerable differences in the ratio of the *gag* gene proteins to pp60^{src}. The autoradiograms were scanned, and the distribution of label in the *gag* protein p27 (the fastest-migrating *gag* protein in Fig. 1), *env* protein precursor gPr92^{env}, and pp60^{src} were obtained. From these data it was determined that two to three times more total viral protein accumulated in the PrB-infected cells than in either the PrA- or the PrC-infected cells during the 5-h labeling period (data not shown). Also, the ratio of pp60^{src} to p27 was approximately twofold higher in the PrA- and PrB-infected cells than in the PrC-infected cells. The absolute levels of pp60^{src} were also higher in the PrA and PrB versus PrC RSV-infected cells. The observed differences in the transformed phenotype therefore correlated with the relative accumulation rates of pp60^{src} in the cells.

Synthesis and splicing of viral RNA. The observed differences in accumulation of viral protein in infected cells might be explained by differences in the respective viral mRNA levels. To examine this possibility, we carried out RNA dot blots by using various amounts of total RNA from infected cells. The PrB-infected cells contained two to four times as much total steady-state viral RNA in comparison with the PrA- and PrC-infected cells (data not shown). These results are consistent with the protein synthesis results which indicated a two- to threefold increase in accumulation of viral protein in PrB-infected cells. To determine the steady-state distribution of the various spliced and unspliced RNA species, equal amounts of RNA from each of the types of infected cells were electrophoresed on formaldehyde-containing agarose gels, blotted onto nitrocellulose, and hybridized with a ^{32}P-labeled viral DNA probe (Fig. 2). Since the PrB-infected cells contained a larger proportion of the cellular RNA as viral RNA, we show two exposure times (48 h in Fig. 2A and 7 days in Fig. 2B) of the autoradiogram to directly compare the RNA ratios in the PrC- and PrA-infected cells with those in the PrB-infected cells. It was clear from these results that there were significant differences in the steady-state ratios of unspliced 9.3-kb RNA to spliced 2.7-kb *src* gene mRNA. The film shown in Fig. 2B was overexposed to show the difference in the steady levels of *src* mRNA in the PrA and PrC strains. Cells infected with either the PrB or the PrA strains contained relatively more 2.7-kb *src* mRNA in comparison with the 9.3-kb RNA than did those cells infected with the PrC strain.

These differences in steady-state ratios could result either from differences in the extent of splicing of the 9.3-kb RNA or in the differential stabilities of the various RNA species. To examine the latter point, we analyzed hybrid-selected viral RNA which had been labeled for either 3 or 12 h with

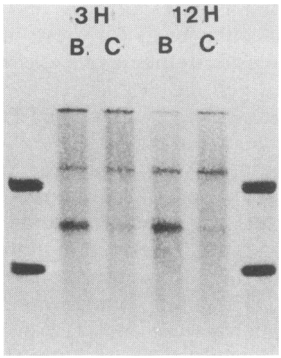

FIG. 3. Comparison of [^{3}H]uridine-labeled hybrid-selected RNA from PrB and PrC RSV-infected cells. [^{3}H]uridine-labeled poly(A)$^+$ RNA from infected cells labeled for 3 or 12 h was hybrid selected and analyzed by formaldehyde-agarose gel electrophoresis by procedures described in the text. Approximately 2×10^4 cpm was applied to each lane. The two outside lanes are markers, [^{3}H]uridine-labeled CEF rRNA.

[^{3}H]uridine (Fig. 3). It was apparent from this experiment that the relative amounts of spliced 2.7-kb *src* mRNA synthesized in a 3-h period was considerably reduced in the PrC-infected cells when compared with the PrB-infected cells. Similar results were obtained when viral RNA labeled for 3 h was selected from PrA- and PrC-infected cells (data not shown). These results agreed with the results of the steady-state RNA distributions shown in Fig. 3. Therefore, if the observed differences in levels of *src* mRNA were due to RNA stability, the half-life of the PrC *src* mRNA would be expected to be shorter than 3 h and considerably different from the PrB and PrA *src* mRNAs. To determine if differential turnover of *src* gene mRNA might account for the results, we treated infected cells with 1 μg of actinomycin D per ml to block further accumulation of viral RNA and then harvested RNA at zero time and at 3-h intervals thereafter. The results of this experiment are given in Fig. 4. Note that the *src* gene mRNA is relatively stable in both PrA- and PrC-infected cells, and the half-life appeared to be longer than 3 h. These data are consistent with previous results obtained for the B77 strain of RSV in which a half-life of approximately 9 h was obtained for the *src* mRNA (30). Previous results have indicated that, under certain conditions, high concentrations of actinomycin D alter the stability of mRNA (8). However, we have shown in a previous study that the half-life of the RSV 9.3-kb RNA determined by the 1-μg/ml actinomycin D blockade was similar to the value obtained by both pulse-chase and approach-to-isotopic-equilibrium methods (30). The results therefore suggest but do not prove that the different steady-state RNA distributions exhibited by the various RNA variants are due to different efficiencies of splicing rather than to a rapid turnover of the *src* mRNA in the PrC-infected cells.

Construction and characterization of recombinants between PrA and PrC RSVs. The above results suggested that there were distinct genetic differences among the different virus isolates in the efficiency of RNA splicing. To determine the genetic element(s) responsible for these differences, we constructed a number of recombinant pBR322-based DNA plasmids in which sequences from low-splicing-efficiency genomes were exchanged with high-efficiency genomes. We used infectious plasmids of PrA and PrC (pJD100 and pATV-8, respectively) (Fig. 5) since infected cells of both viruses contained comparable amounts of viral RNA (Fig. 2), and therefore the results should not be affected by differences in intracellular RNA concentrations. The construction of the clones is diagrammed in Fig. 5. Each of these clones was characterized by restriction enzyme digests and demonstrated the appropriate diagnostic PrC restriction sites. These clones were introduced into parallel cultures of CEF by calcium phosphate transfection techniques. Several cell passages were required to ensure that the cells were completely infected. The results (Fig. 6) indicated that, in cells transfected with plasmid p5′C-3′A, precursors appear to be spliced to *src* gene mRNA with the same high efficiency as the parental PrA plasmid pJD100, whereas in cells transfected with plasmid p5′A-3′C, the extent of splicing to *src* mRNA was similar to the wild-type PrC-infected cells. These results indicate that sequences in the 3′ one-third of the genome determine the level of spliced *src* mRNA. The relative level of splicing of the *env* mRNA appeared to be similar in all cases, and this was borne out by densitometric measurements of the autoradiogram (data not shown).

To further define the region responsible for the effects on splicing, we constructed an additional mutant (pJD100Nco2) in which only the noncoding sequence of pJD100 (PrA) between the *Sac*I site at nucleotide 6865 and the *Nco*I site at 7147 was replaced by PrC sequences (Fig. 5). A transfection experiment similar to the experiment described above was carried out, and the RNAs from cells transfected with pJD100, pATV-8, p5′C-3′A, p5′A-3′C, and pJD100Nco2 were compared by Northern blot analysis (Fig. 7). Three different concentrations of RNA were run for each type of virus; representative examples for each are shown. This experiment showed that pJD100Nco2 (Fig. 7, lane 2) demonstrated a splicing phenotype similar to the wild-type pATV-8 (Fig. 7, lane 3) and p5′A-3′C (Fig. 7, lane 4). As shown in the previous experiment, p5′C-3′A-transfected cells (Fig. 7, lane 5) demonstrated a similar RNA profile to that of the wild-type PrA clone, pJD100 (Fig. 7, lane 6). The autoradiogram was scanned, and the results indicated that

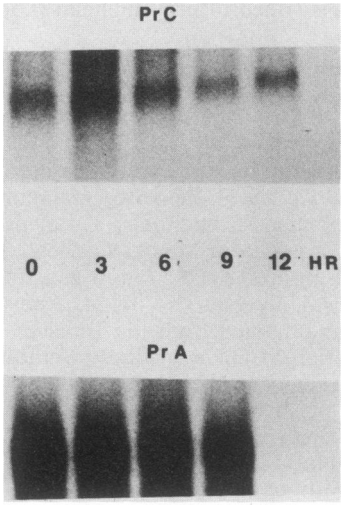

FIG. 4. Comparison of *src* mRNA turnover in cells infected with PrC or PrA RSV. Cells infected with either PrC or PrA RSV were treated with medium containing 1 μg of actinomycin D per ml for various times. At each time point (0, 3, 6, and 9 h for PrA; 0, 3, 6, 9, and 12 h for PrC), total RNA was isolated from parallel cultures and analyzed by Northern blot analysis. The probe was an internal *src* fragment labeled by nick translation with ^{32}P. Only the *src* mRNA band is shown. Autoradiography was carried out for 6 h.

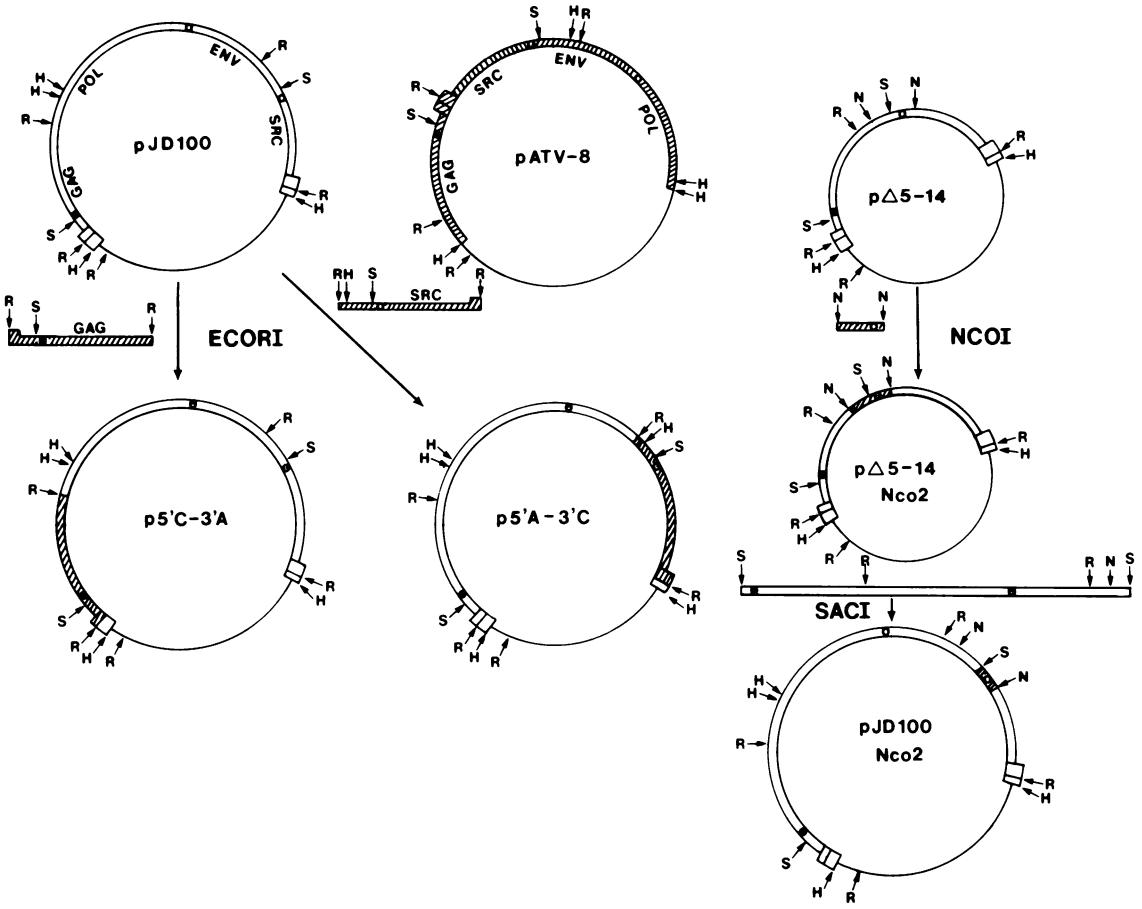

FIG. 5. Construction of recombinant virus plasmids. This figure shows the structures of the plasmids used in the experiments described in the text and the cloning procedures. pΔ5-14 was obtained by partial cleavage of pJD100 with *Xho*I followed by religation and is deleted from nucleotides 630 to 5258. Plasmid pΔ5-14Nco2 was obtained by complete cleavage of pΔ5-14 with *Nco*I and insertion of the indicated *Nco*I-*Nco*I fragment (nucleotides 6529 to 7127) from pATV-8. Infectious plasmid pJD100Nco2 was then constructed by insertion of the indicated *Sac*I-*Sac*I fragment (nucleotides 255 to 6865) from pJD100 into pΔ5-14Nco2. R, *Eco*RI; H, *Hin*dIII; S, *Sac*I; N, *Nco*I. Symbols: ●, donor splice site; ○, acceptor splice site. PrC sequences are shown as hatched regions, and PrA sequences are shown as open regions. The single line denotes pBR322 sequences which are in the same orientation in both the permuted pATV-8 and pJD100 plasmids.

the ratio of 2.7-kb *src* mRNA to 9.3-kb unspliced RNA of pJD100Nco2 was similar to the wild-type PrC clone as well as to p5'A-3'C. However, cells infected with the wild-type PrA clone, pJD100, or p5'C-3'A demonstrated a two- to threefold increase in the relative amount of *src* mRNA. There was less difference among the different clones in the relative amounts of *env* mRNA; however, it is not yet clear whether there are subtle differences in the extent of *env* splicing among the different mutants. We concluded from these experiments that the exchange between PrC and PrA of the 262-nucleotide sequence between the *env* and the *src* genes was sufficient to determine the lowered relative amount of *src* splicing observed in the PrC-infected cells.

Comparison of nucleotide sequences of PrA and PrC RSVs in the region between *env* and *src*. The previous results indicated that the sequences determining the splicing efficiency of PrA versus PrC RSV resided in the noncoding region between the *env* and *src* genes. To begin to understand the mechanisms responsible for generating the observed differences in splicing efficiency, we determined the nucleotide sequence of pJD100 between the *Sac*I and the *Nco*I sites (Fig. 8) and compared it with the published sequence of pATV-8 (26). Only four nucleotide differences were found (Fig. 8). Two of the differences are within the *src* gene intron (we confirmed these differences in our laboratory), and two are in the *src* gene exon. Three are transitions: C to T at nucleotide 6957, A to G at nucleotide 7059, and G to A at nucleotide 7074. There is also a deletion of an A at nucleotide 7023.

DISCUSSION

We have shown in this paper that different cloned variants of Prague RSV vary in the efficiencies of splicing at the *src* gene 3' splice site resulting in two- to threefold differences in the relative amounts of $pp60^{src}$ accumulation in the infected cells. Differences among a number of avian sarcoma and leukosis viruses in the ratio of spliced to unspliced RNA have previously been reported (15). However, it was not clear from these results if the steady-state differences were due to splicing or to differential RNA stabilities. The evidence presented in this paper suggests but does not prove that the differences we observed are due to splicing.

The location of the sequences determining the efficiency of splicing to the region immediately upstream from the *src* 3' splice site may help to explain a puzzling observation previously reported by Tsichlis and Coffin (34). Transformation-competent recombinants between PrB RSV and

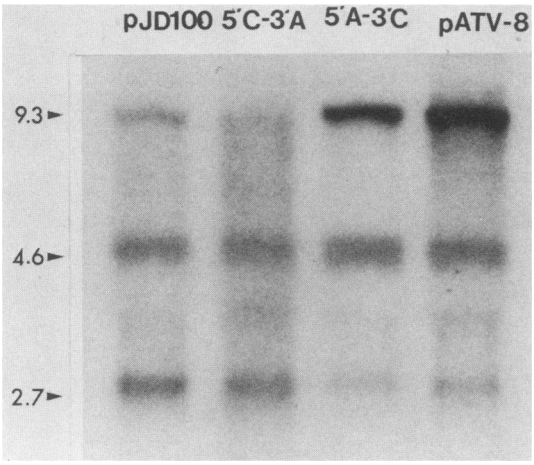

FIG. 6. Northern blot analysis of RSV RNA from cells transfected with wild-type and recombinant plasmids. CEF were transfected as described in the text. Total RNA from infected cells was isolated. Samples of RNA (10 μg) were applied to formaldehyde-agarose gels, the gel was blotted onto nitrocellulose, and the filter was hybridized to a ^{32}P-labeled probe. Equivalent amounts of RNA from each were applied and transferred as monitored by ethidium bromide staining of the rRNA bands. This probe was prepared by nick translation of a restriction fragment from the *src* gene coding sequence. Autoradiography was carried out for 17 h.

nontransforming Rous-associated virus-0 were examined by oligonucleotide mapping. Whereas most of the sequences outside the selected *env* gene from Rous-associated virus-0 appeared to recombine at high levels between the two types of viruses, several other regions of the transforming PrB RSV also were consistently from the PrB parent. One of

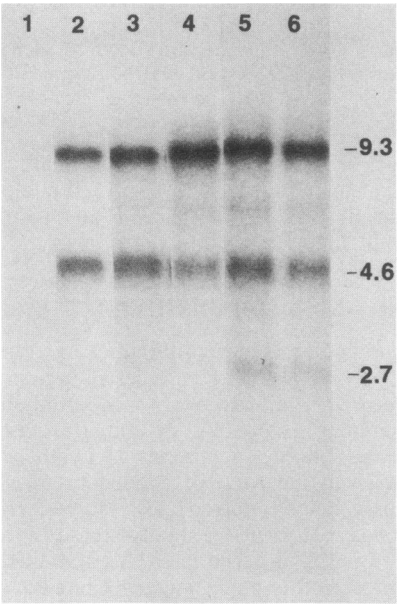

FIG. 7. Further Northern blot analysis of various RSV RNAs. The protocol described in the legend to Fig. 6 was also used in this experiment. Lanes: 1, uninfected control; 2, cells transfected with pJD100Nco2; 3, cells transfected with pATV-8; 4, cells transfected with p5'A-3'C; 5, cells transfected with p5'C-3'A; 6, cells transfected with pJD100. Autoradiography was carried out for 19 h.

```
              *** gp 35 ends      .6880      .          .          .
PrC     CAGTCTAGAGAGCTCAGTTATAATAATCCTGCGAATCGGGCTGTAACGGGGCAAG
PrA     ------------------------------------------------------

                  .          .6930      .          .          .
        GCTTGACCGAGGGGACTATAACATGTATAGGCGAAAAGCGGGGTCTCGGTTGTAA
        ---------------------------------------------T--------

          .          .          .          .7000      .          .
        CGCGCTTAGGAAGTCCCCTCGAGGTATGGCAGATATGCTCTTGCATAGGGGGAAA
        ------------------------------------------------------

                  .          .7040      .  ↓       .          .
        AAATGTAGTCTTAATATTGTCTGTGTGCTGCAGGAGCTAAGCTGACTCTGCTGGT
        --\-----------------------------------G----------------
          del                           3' splice site

          .          .7090      .          .  pp60src begins  **
        GGCCTCGCGTACCACTGTGGCCAGGCGGTAGCTGGGACGTGCAGCCGACCACCAU
        --------A---------------------------------------------
```

FIG. 8. Complete nucleotide sequence of the 262-base-pair noncoding region between *Sac*I and *Nco*I of pJD100 (PrA) compared with the same region of pATV-8 (PrC). Numbering is according to data of Schwartz et al. (26). Symbols: −, both strains are similar at a given position; \, deletion of specific bases. The splice acceptor site is shown as a vertical arrow.

these regions was immediately upstream from the *src* 3′ splice site and included the sequences which we defined in this study.

The nature of the *cis*- and *trans*-acting viral or cellular factors that govern the levels of spliced and unspliced retrovirus RNAs has not yet been clearly established. Evidence has previously been obtained suggesting a role for the avian retroviral *gag* gene protein p19 as a possible *trans*-acting factor that binds to the RNA near the 5′ and 3′ splice sites and thus prevents splicing (14, 15). The data presented in this paper suggest that the differences we saw in the splicing efficiencies of PrA versus PrC RSV were not due to the binding affinities of the respective p19 proteins since the recombinant virus (p5′C-3′A) containing the PrC RSV *gag* gene (derived from plasmid pATV-8) appears to have the same efficiency of *src* splicing as does the wild-type PrA virus (derived from pJD100). Another hypothesis which has been previously proposed is that internal adenosine methylations of the RNA play a role in determining the levels of spliced and unspliced RNA (29). Methylation differences, however, do not appear to explain the results obtained above since the region that appears to determine the extent of *src* gene splicing, i.e., between the *env* and *src* genes, has been shown not to be specifically methylated in the RSV genome RNA (10), and there were no sequence differences between the PrA and PrC genomes (Fig. 8) at potential mRNA methylation sites (4, 10). A third and more reasonable possibility is that the splicing efficiencies observed here were due to differences in the affinities of the RNAs for cellular or virus-encoded splicing factors. The results in this paper suggest that the virus element(s) acts in *cis*, an expected result for such a model. Furthermore, the observation that the sequences surrounding the 3′ splice acceptor site determine that the splicing efficiency is consistent with a recent report, suggesting that the initial interaction of RNA with the splicing machinery occurs at the 3′ splice site (24). Therefore, any interference with the formation of the splicing complex at the 3′ site may inhibit splicing.

How would such interference occur? One possibility is that the secondary structure of the RNA in the region of the 3′ splice site may inhibit the interaction of the splicing machinery with the 3′ splice site and the formation of the lariat intermediate. Evidence obtained from in vitro splicing

experiments has indicated that RNA secondary structure can play a negative role in splicing by sequestering 3′ splice sites in duplex regions (28). Evidence consistent with the role of long-range RNA interactions in retrovirus RNA splicing has also been obtained. The introduction of a certain foreign sequence into the *env* gene intron of reticuloendotheliosis virus, even at sites removed from the splice junction, reduces the amount of splicing at the *env* 3′ splice site (20). Deletions within the Moloney murine leukemia virus *env* gene intron can dramatically affect the levels of spliced mRNA, again suggesting that a long-range effect of RNA conformation may alter splicing efficiency (9).

We carried out a computer analysis of the region between the Prague *env* and *src* genes by using a program developed by M. Zuker, and the data indicated that several stem-loop structures may exist in this region which may affect splicing. The presence of such structures is consistent with the observed sensitivity of this region to digestion by RNase III (3). We still understand little about the effects of 1-base changes on RNA secondary structure, and therefore the result of the sequence differences between PrA and PrC RSVs on the secondary structure of their RNAs is difficult to predict.

Another possible explanation for the effect of the sequence differences is that they affect the binding of viral *gag* proteins. It is of interest that the 1-base deletion at nucleotide 7023, 30 bases upstream from the *src* 3′ splice site, is part of a sequence which was predicted to be a p19 binding site by Darlix and Spahr (3). (Recent evidence, however, suggests that these may actually be sites for binding of p12 [19].) Since this nucleotide is in a 12-base run of purines (Fig. 8), it would be surprising if such a subtle change would significantly affect *gag* protein binding. However, this is also a region of the *src* gene intron where a lariat intermediate branch point might be expected to form (22, 25), and the possible interaction or overlap of these sites may be of importance in explaining the effect on splicing. The change at nucleotide 7059 (A to G transition) is 6 bases downstream from the 3′ splice site in the *src* gene exon. It is conceivable that this region may also affect splicing efficiency since certain 1-base exon mutations (at the 5′ end of the exon) have recently been shown to influence the splicing of Chinese hamster ovary cell dihydrofolate reductase mRNA (21). It is of interest that a G rather than an A is also present at this position in the PrB RSV (1), the Schmidt-Ruppin A RSV (2), and the chicken c-*src* mRNA (33). Further work is under way to determine which of the observed sequence changes are associated with the altered splicing phenotype.

ACKNOWLEDGMENTS

This research was supported by Public Health Service grant CA-28051 from the National Cancer Institute.

We thank Mark Stinski and Bill Goins for critically reading the manuscript and Marcia Reeve for typing the manuscript.

LITERATURE CITED

1. **Chang, L.-J., and C. M. Stoltzfus.** 1985. Cloning and nucleotide sequences of cDNAs spanning the splice junctions of Rous sarcoma virus mRNAs. J. Virol. **53**:969–972.
2. **Czernilofsky, A. P., A. D. Levinson, H. E. Varmus, J. M. Bishop, E. Tischler, and H. M. Goodman.** 1983. Corrections to the nucleotide sequence of the *src* gene of Rous sarcoma virus. Nature (London) **301**:736–738.
3. **Darlix, J.-L., and P. F. Spahr.** 1982. Binding sites of viral protein p19 onto Rous sarcoma virus RNA and possible controls of viral functions. J. Mol. Biol. **160**:147–161.
4. **Dimock, K., and C. M. Stoltzfus.** 1977. Sequence specificity of internal methylation in B77 avian sarcoma virus RNA subunits. Biochemistry **16**:471–478.
5. **Ficht, T. A., L.-J. Chang, and C. M. Stoltzfus.** 1984. Avian sarcoma virus *gag* and *env* gene structural protein precursors contain a common amino-terminal sequence. Proc. Natl. Acad. Sci. USA **81**:362–366.
6. **Graham, F. L., and A. J. van der Eb.** 1973. A new technique for the assay of infectivity of human adenovirus 5 DNA. Virology **52**:456–467.
7. **Hackett, P. B., R. Swanstrom, H. E. Varmus, and J. M. Bishop.** 1982. The leader sequence of the subgenomic mRNA's of Rous sarcoma virus is approximately 390 nucleotides. J. Virol. **41**:527–534.
8. **Herman, R. C., and S. Penman.** 1977. Multiple decay rates of heterogeneous nuclear RNA in HeLa cells. Biochemistry **16**:3460–3465.
9. **Hwang, L.-H. S., J. Park, and E. Gilboa.** 1984. Role of intron-contained sequences in the formation of Moloney murine leukemia virus *env* mRNA. Mol. Cell. Biol. **4**:2289–2297.
10. **Kane, S. E., and K. Beemon.** 1985. Precise localization of m^6A in Rous sarcoma virus RNA reveals clustering of methylation sites: implications for RNA processing. Mol. Cell. Biol. **5**:2298–2306.
11. **Katz, R. A., C. A. Omer, J. H. Weis, S. A. Mitsialis, A. J. Faras, and R. V. Guntaka.** 1982. Restriction endonuclease and nucleotide sequence analyses of molecularly cloned unintegrated avian tumor virus DNA: structure of large terminal repeats in circle junctions. J. Virol. **42**:346–351.
12. **Kessler, S. W.** 1975. Rapid isolation of antigens from cells with a staphlococcal protein A-antibody adsorbent: parameters of the interaction of antibody-antigen complexes with protein A. J. Immunol. **115**:1617–1624.
13. **Laemmli, U. K.** 1970. Cleavage of structural proteins during the assembly of the head of bacteriophage T4. Nature (London) **227**:680–685.
14. **Leis, J. P., J. McGinnis, and R. W. Green.** 1978. Rous sarcoma virus p19 binds to specific double-stranded regions of viral RNA: effect of p19 on cleavage of viral RNA by RNase III. Virology **84**:87–98.
15. **Leis, J. P., P. Scheible, and R. E. Smith.** 1980. Correlation of RNA binding affinity of avian oncornavirus p19 proteins with the extent of processing of virus genome RNA in cells. J. Virol. **35**:722–731.
16. **Lowry, O. H., N. J. Rosebrough, A. L. Farr, and P. J. Randall.** 1951. Protein measurement with the Folin phenol reagent. J. Biol. Chem. **193**:265–275.
17. **Maniatis, T. E., E. F. Fritsch, and J. Sambrook.** 1982. Molecular cloning: a laboratory manual. Cold Spring Harbor Laboratory, Cold Spring Harbor, N.Y.
18. **Maxam, A. M., and W. Gilbert.** 1980. Sequencing end-labeled DNA with base-specific chemical cleavages. Methods Enzymol. **65**:499–560.
19. **Meric, C., J.-L. Darlix, and P.-F. Spahr.** 1984. It is Rous sarcoma virus protein p12 and not p19 that binds tightly to Rous sarcoma virus RNA. J. Mol. Biol. **173**:531–538.
20. **Miller, C. K., and H. M. Temin.** 1986. Insertion of several different DNAs in reticuloendotheliosis virus strain T suppresses transformation by reducing the amount of subgenomic mRNA. J. Virol. **58**:75–80.
21. **Mitchell, P. J., G. Urlaub, and L. Chasin.** 1986. Spontaneous splicing mutations at the dihydrofolate reductase locus in Chinese hamster ovary cells. Mol. Cell. Biol. **6**:1926–1935.
22. **Padgett, R. A., M. M. Konarska, P. J. Grabowski, S. F. Hardy, and P. A. Sharp.** 1984. Lariat RNA's as intermediates and products in the splicing of messenger RNA precursors. Science **225**:898–903.
23. **Rigby, P. W. J., M. Dieckman, C. Rhodes, and P. Berg.** 1977. Labeling deoxyribonucleic acid to high specific activity in vitro by nick translation with DNA polymerase I. J. Mol. Biol. **113**:237–251.
24. **Ruskin, B., and M. R. Green.** 1985. Specific and stable intron-factor interactions are established early during in vitro pre-mRNA splicing. Cell **43**:131–142.
25. **Ruskin, B., A. R. Krainer, T. Maniatis, and M. R. Green.** 1984.

Excision of an intact intron as a novel lariat structure during pre-mRNA splicing in vitro. Cell **38**:317–331.

26. **Schwartz, D. E., R. Tizard, and W. Gilbert.** 1983. Nucleotide sequence of Rous sarcoma virus. Cell **32**:853–869.
27. **Sefton, B. M., K. Beemon, and T. Hunter.** 1978. Comparison of the expression of the *src* gene of Rous sarcoma virus in vitro and in vivo. J. Virol. **28**:957–971.
28. **Solnick, D.** 1985. Alternative splicing caused by RNA secondary structure. Cell **43**:667–676.
29. **Stoltzfus, C. M., and R. W. Dane.** 1982. Accumulation of spliced avian retrovirus mRNA is inhibited in *S*-adenosylmethionine-depleted chicken embryo fibroblasts. J. Virol. **42**:918–931.
30. **Stoltzfus, C. M., K. Dimock, S. Horikami, and T. A. Ficht.** 1983. Stabilities of avian sarcoma virus RNAs: comparison of subgenomic and genomic species with cellular mRNAs. J. Gen. Virol. **64**:2191–2202.
31. **Strohman, R., P. Moss, J. Micou-Eastwood, D. Spector, A. Przybyla, and B. Peterson.** 1977. Messenger RNA for myosin polypeptides: isolation from single myogenic cell cultures. Cell **10**:265–273.
32. **Swanstrom, R., R. C. Parker, H. E. Varmus, and J. M. Bishop.** 1983. Transduction of cellular oncogenes: the genesis of Rous sarcoma virus. Proc. Natl. Acad. Sci. USA **80**:2519–2523.
33. **Takeya, T., and H. Hanafusa.** 1983. Structure and sequence of the cellular gene homologous to the RSV *src* gene and the mechanism for generating transforming virus. Cell **32**: 881–890.
34. **Tsichlis, P. N., and J. M. Coffin.** 1980. Recombinants between endogenous and exogenous avian tumor viruses: role of the C region and other portions of the genome in the control of replication and transformation. J. Virol. **33**:238–249.
35. **Varmus, H., and R. Swanstrom.** 1982. Replication of retroviruses, p. 369–512. *In* R. Weiss, N. Teich, H. Varmus, and J. Coffin (ed.), RNA tumor viruses: molecular biology of tumor viruses. Cold Spring Harbor Laboratory, Cold Spring Harbor, N.Y.